

## Luminescence chronology and facies development of Bhur sands in the interfluvial region of Central Ganga Plain, India

Pradeep Srivastava<sup>†,‡</sup>, Uma Kant Shukla<sup>#</sup>,  
Praveen Mishra<sup>‡</sup>, Maneesh Sharma<sup>†</sup>,  
Shikha Sharma<sup>†</sup>, I. B. Singh<sup>†</sup> and  
A. K. Singhvi<sup>†,\*</sup>

<sup>†</sup>Department of Geology, Lucknow University,  
Lucknow 226 007, India

<sup>‡</sup>Earth Science Division, Physical Research Laboratory,  
Ahmedabad 380 009, India

<sup>#</sup>Department of Geology, Kumaun University,  
Nainital 263 002, India

**Bhur sand ridges in the upland interfluvial surface are a distinctive feature of the Ganga Plain and occur as arcuate, linear and oval geomorphic highs. Their sedimentary sequence shows a few meter thick aeolian sand cover invariably underlain by fluvial channel deposits in the form of point bar succession. Infra-red stimulated luminescence (IRSL) dating of the topmost part of the channel sand and the overlying aeolian sediments yielded stratigraphically consistent results and indicated that the fluvial channel activity in the region ceased sometime during 7 to 5 ka. This was followed by a phase of deposition of aeolian sand, suggesting a phase of weakened monsoon and increased aridity.**

THE Ganga Plain is a part of Himalayan foreland basin where fluvial sedimentation has been the dominant

sedimentation process since the Middle Miocene<sup>1-5</sup>. It is considered that distinctive geomorphic features such as upland interfluvial surfaces (terrace-T<sub>2</sub>), river valley terrace (terrace-T<sub>1</sub>), present-day flood plain (terrace-T<sub>0</sub>), alluvial ridges and ponds in the alluvial plains formed in response to the climate and associated sea-level changes during the Late Quaternary<sup>5</sup>. Upland interfluvial surface, the most prominent geomorphic feature of the Ganga Plain constitutes a topographic high, in which major rivers and their valleys are entrenched. It has been suggested that these surfaces began accreting since the last interglacial (~128 ka) (ref. 5).

The Central Ganga Plain shows extensive development of interfluvial surfaces with relict alluvial landforms such as abandoned channels, alluvial ridges, abandoned meander belts, etc.<sup>6</sup>. Alluvial ridges (termed as Bhur sand deposits) occur on the upland interfluvial surfaces as stabilized sandy mounds and comprise oxidized, brown-yellow, fine to medium grained micaceous sand<sup>7</sup>. Earlier workers mapped Bhur sands/alluvial ridges as aeolian deposits. However, some workers like Pandey *et al.*<sup>8</sup> consider these as older fluvial sands partly reworked by aeolian agencies.

The present study is aimed to characterize the facies, geometry, the mode of occurrence and chronology of alluvial ridges at Gahira Bypass and near Gangaganj described previously by Singh *et al.*<sup>9</sup>. Figure 1 shows some of the shapes of alluvial ridges seen commonly in the Western Ganga Plain. The oval ridges that occur in clusters are smaller in size with a relief of ~2 m, width 50–75 m and are traceable up to 250 m. The linear ridges have a relief of 2–5 m, width 50–200 m and are traceable for 0.5–2.5 km. The arcuate ridges occur as fragments of abandoned meander belt with a relief of

\*For correspondence. (e-mail: Singhvi@prl.ernet.in)

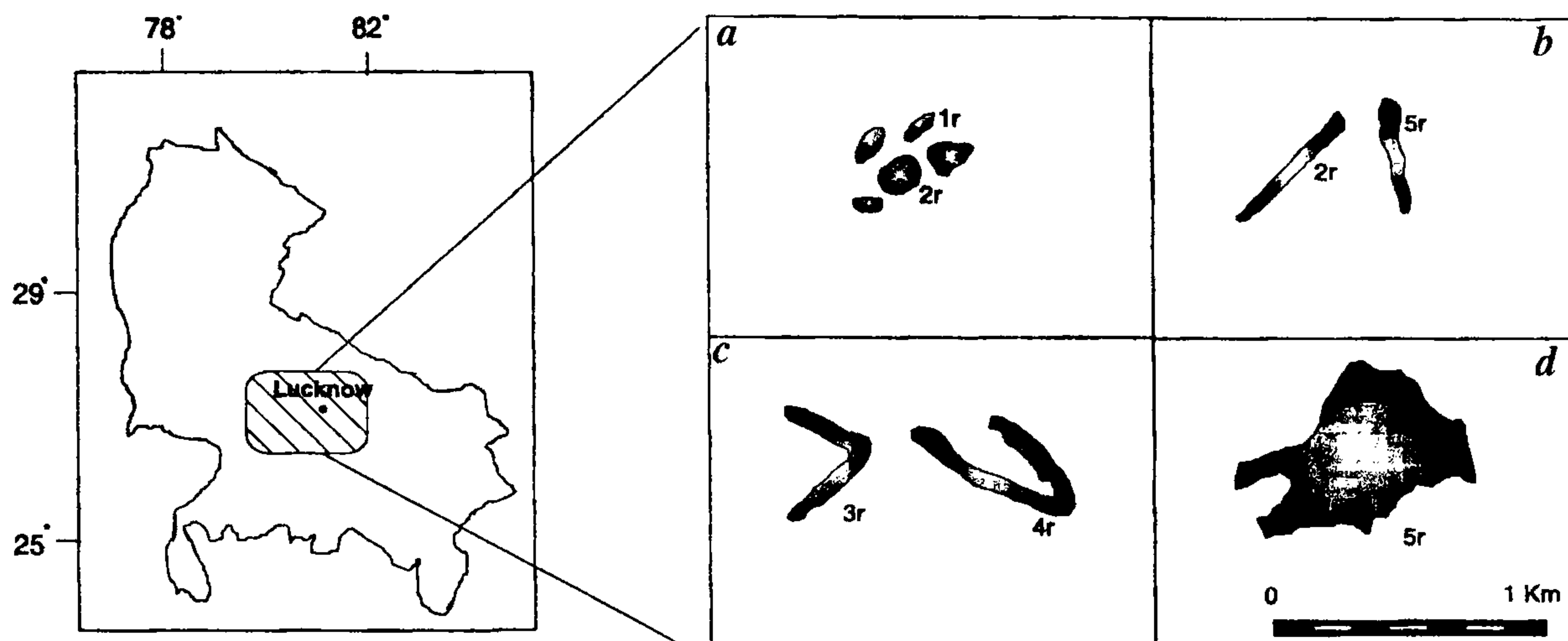


Figure 1. Types of alluvial ridges. *a*, Oval; *b*, Linear; *c*, Arcuate; *d*, Modified.

Table 1. Lithofacies of alluvial ridge at Gahira bypass

Lithofacies	Thickness (m)	Textural attributes
Cross-bedded sand	0.5–1.5	Grey, large-scale trough and planar cross-bedded, moderate mottling, occasional clay balls
Parallel laminated fine sand	0.5–2.0	Grey-yellow grey, individual laminas 0.5–1.0 cm thick, moderately mottled (Figure 4 <i>a</i> )
Rippled fine sand	0.2–0.3	Grey-yellow grey, present in form of lenses, in different facies. Ripple wavelength $\leq 20.0$ cm and height up to 5.0 cm
Bioturbated fine sand	1.0–3.0	Grey-buff, grey, extensive mottling. Both animal and plant burrows are visible (Figure 4 <i>b</i> )
Well-sorted ferruginized fine sand	1.0–3.0	Yellow-reddish yellow, highly ferruginized, no physical structure but occasional burrows

2–4 m, length ranging from 0.75 to 2.5 km and the sinuosity varying from 2 to 5, suggesting thereby that they were probably part of a highly sinuous abandoned channel. In addition, a few ridges occupy large areas but do not show any specific geometry (Figure 1 *d*).

Detailed study using Survey of India topographical maps in the region of Kali and Ganga rivers (Figure 2) indicated 55 alluvial ridges of linear, arcuate or oval shapes with a positive relief of 2–4 m, suggesting fluvial activity in the past. Average elevation of this area is 176 m above msl and the spot height data suggest an overall inward slope pattern making it a pear-shaped basin. The basin connects to a small perennial channel, which is a part of Nim-nadi, a tributary of Kali river. It is probable that the alluvial ridges occurring within the pear-shaped basin are related to a subwatershed of Nim-nadi. Figure 2 provides reconstruction of palaeo-subwatershed of Nim-nadi. To understand the nature of deposition in Bhur ridges, two such ridges – the Gahira bypass ridge and Gangaganj ridge – were documented for their sedimentary structure.

The Gahira bypass ridge is a 5 m high, 50 m wide alluvial ridge located 19 km from Kanpur on the Kanpur–Lucknow Highway (NH 25) (Figure 3). The ridge comprises channel sand at the base followed by 2–4 m thick aeolian cover of silty sand. The sedimentary

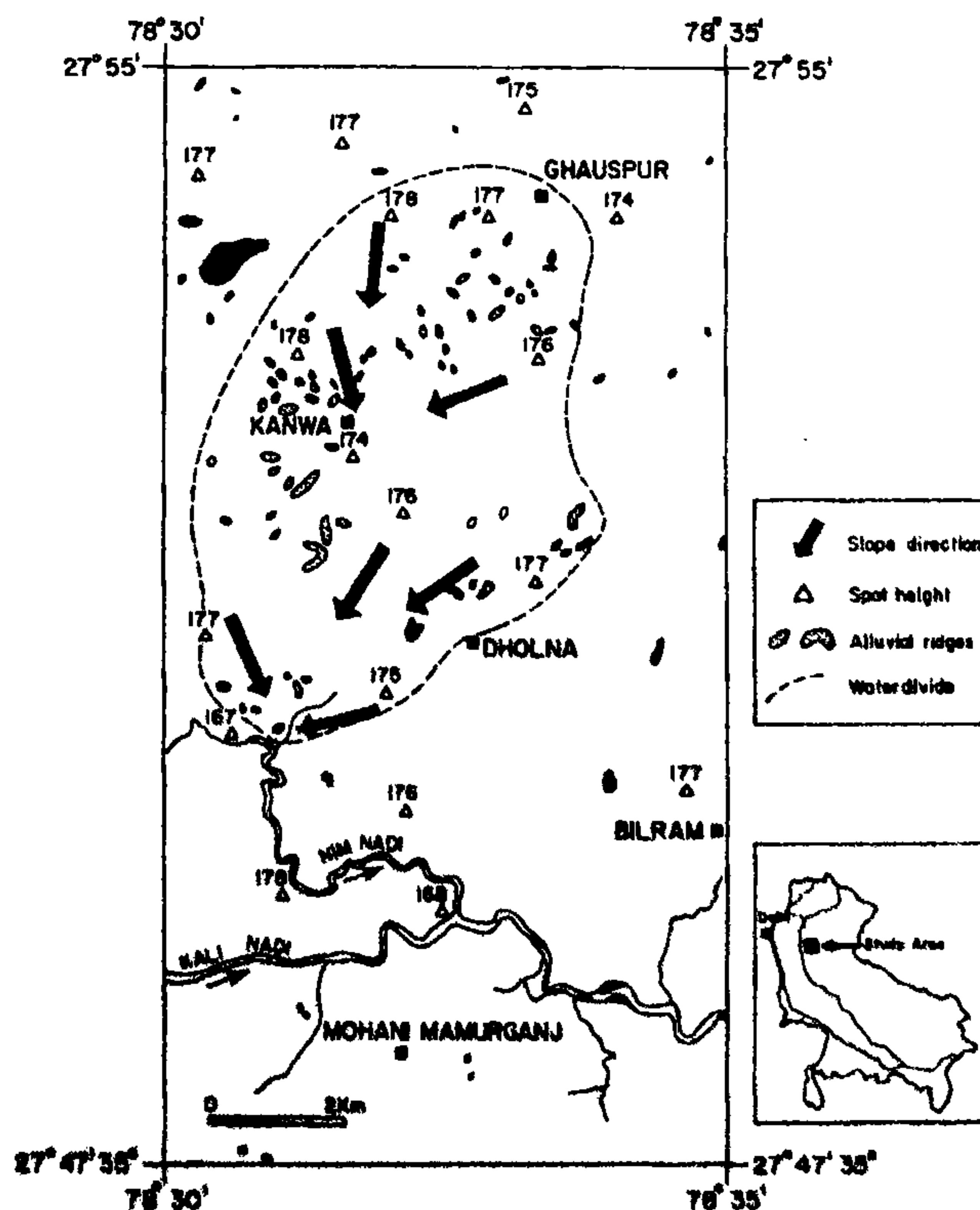


Figure 2. Mode of occurrence of alluvial ridges. Arrows show the pattern of slopes based on the present spot heights. Probable water divide has been demarcated on the basis of change in slopes.

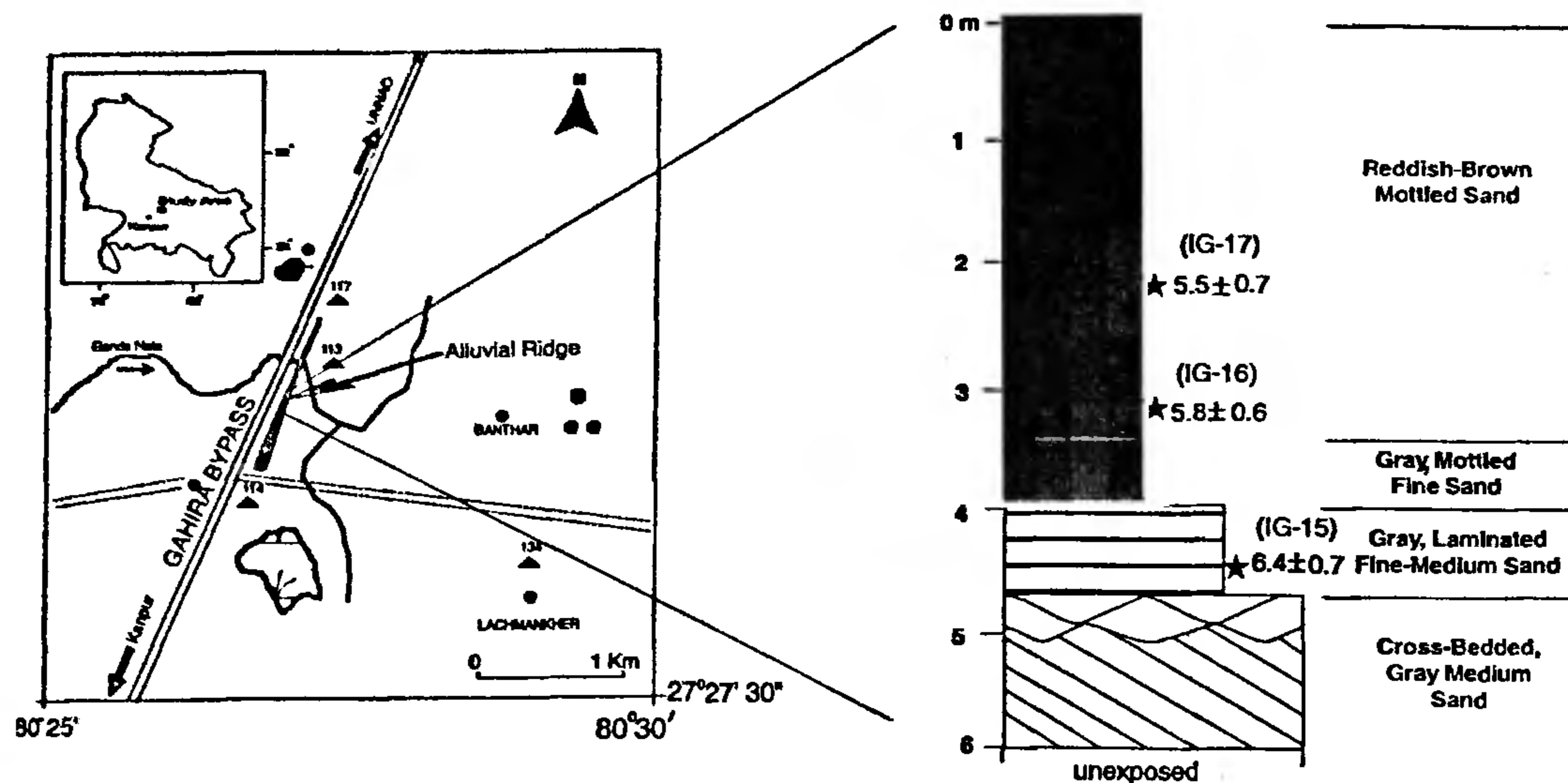


Figure 3. Location map, lithostratigraphy, luminescence ages of alluvial ridge at Gahira bypass.

features were examined by exposing various vertical profiles. An idealized sequence of this ridge is given in Figure 3. The details on lithofacies (from base upwards) are given in Table 1. The sequence from cross-bedded grey sand to bioturbated fine sand is a typical deposit of a channel bar aggradation of a river system. The bar deposits are overlain by well-sorted ferruginized fine sand which represents the initiation of aeolian sedimentation. It is inferred that this ridge was formed primarily by a gradual aggradation of the river bed. Along with the river bed, the levees on both the sides of the channel were also aggraded. This process led the river bed to attain a higher elevation than the adjacent low lying flood plain resulting in a hydraulic disadvantage and consequent abandonment of the channel. This left a linear depression. Due to moisture content in the channel belt, it accreted vertically by trapping aeolian sand and gradually attained a linear ridge-like topography.

The Gangaganj ridge is associated with 3–5 m deep abandoned channel belt. Singh *et al.*<sup>9</sup> identified similar lithofacies as documented in Table 1 in the point bar deposits of this ridge and these are overlain by well-sorted ferruginized aeolian sand. It was also demonstrated that after the final phase of point bar deposition, there was a disruption and abandonment of active channel caused by local tectonic uplift. Presently, the area proximal to this channel is affected by ravine development and patchy appearance of the ravine topography in the area is possibly a consequence of crustal upwarping due to neotectonic activity.

Sediment samples from the alluvial ridge near Gahira bypass and at Gangaganj were luminescence dated. In

general, the chronology of alluvial sediments has been difficult and despite their vast expanse, most of the Gangetic alluvium still remain undated. A limited number of radiocarbon dates of calcrete nodules and shells have been reported but possibilities of contamination during diagenesis<sup>10,11</sup>, difficulties in establishing the exact nature of the sample (autochthonous vs allochthonous) and difficulties of calibration beyond 24 ka do not provide much hope in the use of conventional radiocarbon dating or its recent variant, the accelerator mass spectrometry. In recent years, luminescence dating has been applied extensively to date young sediments<sup>12,13</sup>. Application of luminescence dating method is based on the fact that because of daylight exposure during weathering and transport, the geological luminescence of mineral grains constituting the sediments is reduced to a small value ( $I_0$ ). On burial, further sun exposure ceases and a reaccumulation of the luminescence due to the radiation exposure arising from the decay of natural radioactivity, viz.  $^{232}\text{Th}$ ,  $^{238}\text{U}$  and  $^{40}\text{K}$  present in the sediment starts. There is also a small contribution from the cosmic rays. This reaccumulation of luminescence continues till its excavation. The total luminescence signal ( $I_{\text{nat}}$ ) comprises the initial residual level  $I_0$  and the luminescence ( $I_d$ ) acquired since burial.  $I_d (=I_{\text{nat}} - I_0)$  can be related to age of burial via the annual rate of luminescence induction, i.e.

$$\text{Age} = PID_T,$$

where the equivalent dose or the palaeodose ( $P$ ) represents the laboratory radiation dose that induces a luminescence intensity ( $I$ ) in the sample identical to that in

the natural sample, i.e.  $I_d$ .  $D_T$  represents the total annual radiation dose received by the sample and is computed using the elemental concentrations of natural radioactivity.

An aspect that merits consideration is the estimation of  $I_0$ . Bleaching of luminescence by daylight, of a sample to its residual value, takes up to several hours for thermally stimulated luminescence (TL) and up to several minutes for optically stimulated luminescence (OSL). Aeolian sediments that are transported by wind over long distances and for long time experience direct daylight exposure. This fact enables a reasonable assumption that the geological luminescence of aeolian sediments are bleached to maximum possible extent such that at the time of deposition the grain possessed only a residual level  $I_0$ . However, for fluvially transported sediments net daylight flux available to mineral grains before deposition is significantly attenuated. The extent of bleaching depends on the depth of the water column, turbulence, the grain size and the sediment load, and each of these factors implies a net attenuation of daylight spectrum and flux to the grains<sup>14,15</sup>. Consequently, the extent of bleaching needs to be ascertained in each case.

The advent of OSL dating technique has helped in minimizing some of the problems associated with the dating of fluvial deposits. The primary advantage of OSL dating is that it utilizes light sensitive luminescence traps. This offers certain methodological advantages when dealing with fluvial sediments which possibly experienced only a limited predepositional daylight exposure. In the case of samples from the Gangetic Plains, the feasibility of using infra-red stimulated luminescence dating (IRSL) has been established<sup>16</sup>. Low variability in the IRSL signal of different aliquots also indicates reasonable bleaching of mineral grains in respect of their IRSL.

For luminescence measurements, the samples were sequentially treated with 1N HCl and 30%  $H_2O_2$  to remove carbonates and organics, respectively. These were then sieved to obtain the 125–150  $\mu\text{m}$  grain size fraction. K-rich feldspar fraction was then separated using sodium polytungstate solution (density 2.58  $\text{g}/\text{cm}^3$ ). This fraction was not etched with HF due to possibilities of non-uniform etching. Instead a correction factor was used for the alpha dose to the grain skin. For measurements, a monolayer of feldspar grains was fixed on stainless steel aliquots using *Silkospray*. The measurements were performed on automated TL/OSL reader (Riso TL/OSL-DA-15)<sup>17</sup>. Infra-red stimulation was carried out at 30°C using TEMT-484 diodes emitting at  $880 \pm 80$  nm. Detection optics comprised a EMI 9235 QA photomultiplier tube coupled with Schott BG-39 and Corning 7-59 colour filters. Additive dose technique was used with short shine normalization of 0.3 s and a preheat of 200°C, 1 m. The dose rate was computed using elemen-

tal concentrations of U, Th and K. Thick source ZnS (Ag) alpha counting was employed for the estimation of uranium and thorium. The potassium content was measured using NaI(Tl) gamma ray spectrometry and internal potassium content of grains was assumed to be 12.5%. A cosmic ray dose contribution of  $150 \pm 30$   $\mu\text{Gy}/\text{ka}$  was used<sup>18</sup>. The error computation was done using standard Riso software.

Table 2 provides the experimental data including palaeodose, radioactivity data and age of the samples and Figures 3–5 provide information about the age along with the lithologs. In the case of Gahira bypass ridge samples, IG-15 and IG-17 provided ages of  $6.5 \pm 0.7$  ka and  $5.7 \pm 0.8$  ka, respectively (Figure 3). Maximum age span for this sequence was obtained by adding the experimental error in the lower sample and subtracting the error from the upper sample. This yielded an age upper bound of 7.2 ka for grey fluvial sand and an age lower bound of 4.9 ka for overlying aeolian sand, which suggests that around 7.2 ka the river channel had an active sedimentation phase in form of a channel bar. Subsequently, by around 4.9 ka the channel was already abandoned and became the site for aeolian sedimentation.

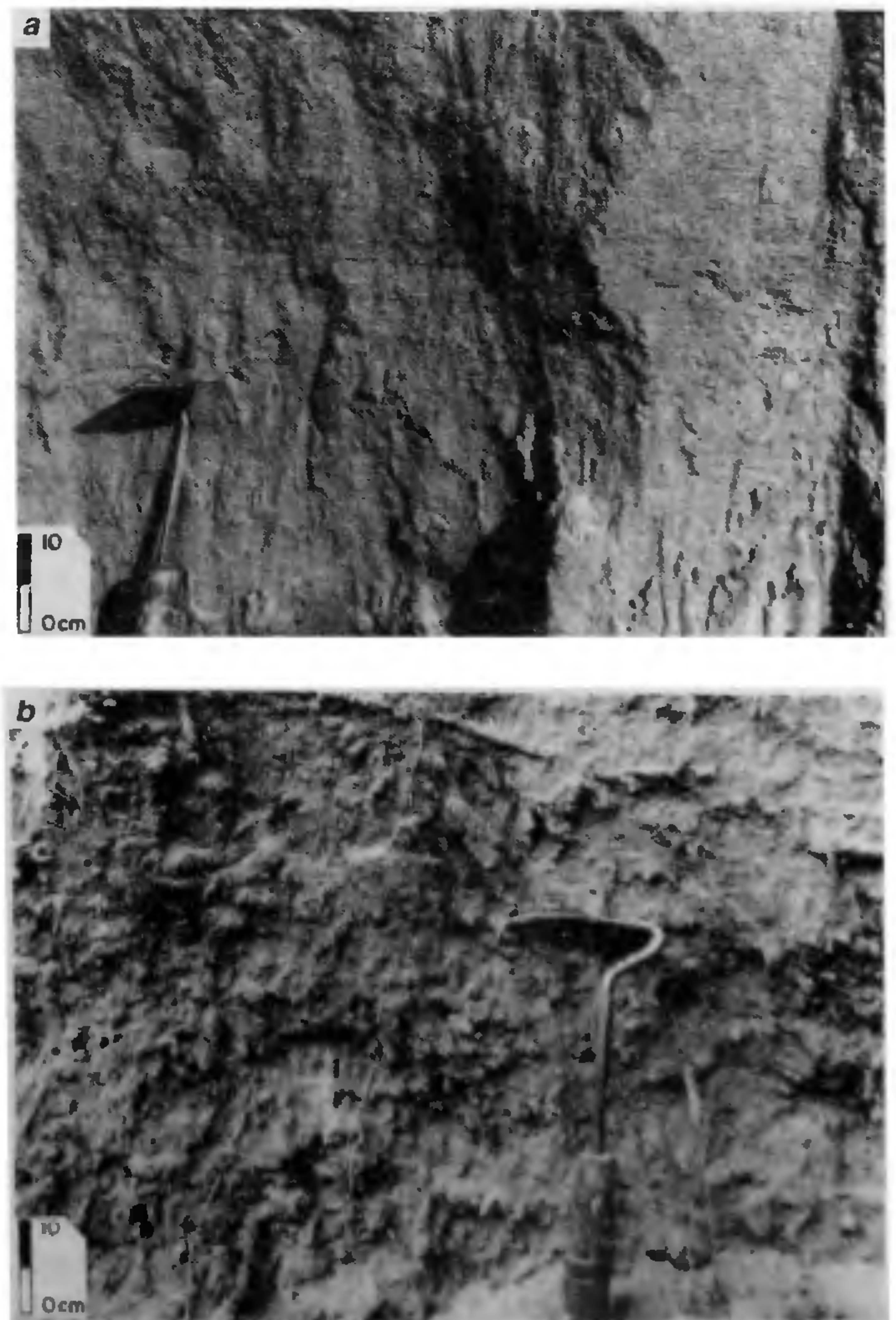


Figure 4. *a*, Parallel laminated fine sand facies; *b*, Bioturbated fine sand facies ridge.

Table 2. Radioactivity, palaeodose and IRSL age estimates

Sample	Depth (m)	U (ppm)	Th (ppm)	K %	Water %	Dose rate (Gy/ka)	Palaeodose (Gy)	Age (ka)
IG-15	4.47	1.8 ± 0.6	10.2 ± 2.0	1.7 ± 0.1	15 ± 5	3.4 ± 0.3	22.0 ± 1.0	6.5 ± 0.7
IG-16	3.12	1.9 ± 0.8	11.5 ± 2.7	2.2 ± 0.1	10 ± 5	4.2 ± 0.4	24.3 ± 0.3	5.8 ± 0.6
IG-17	2.12	2.6 ± 1.4	22.2 ± 5.3	1.8 ± 0.1	10 ± 5	5.0 ± 0.7	28.7 ± 0.1	5.7 ± 0.8
IG-4	0.60	4.5 ± 1.4	19.8 ± 5.0	2.0 ± 0.1	10 ± 5	5.6 ± 0.7	27.6 ± 1.2	5.0 ± 0.7
IG-5	2.08	2.7 ± 1.4	11.7 ± 2.6	2.0 ± 0.1	15 ± 5	4.0 ± 0.5	25.7 ± 2.1	6.4 ± 1.0

Alpha efficiency factor (a value) was assumed to be 0.20 ± 0.05; Cosmic ray contribution was assumed as 150 ± 30 µGy/ka.

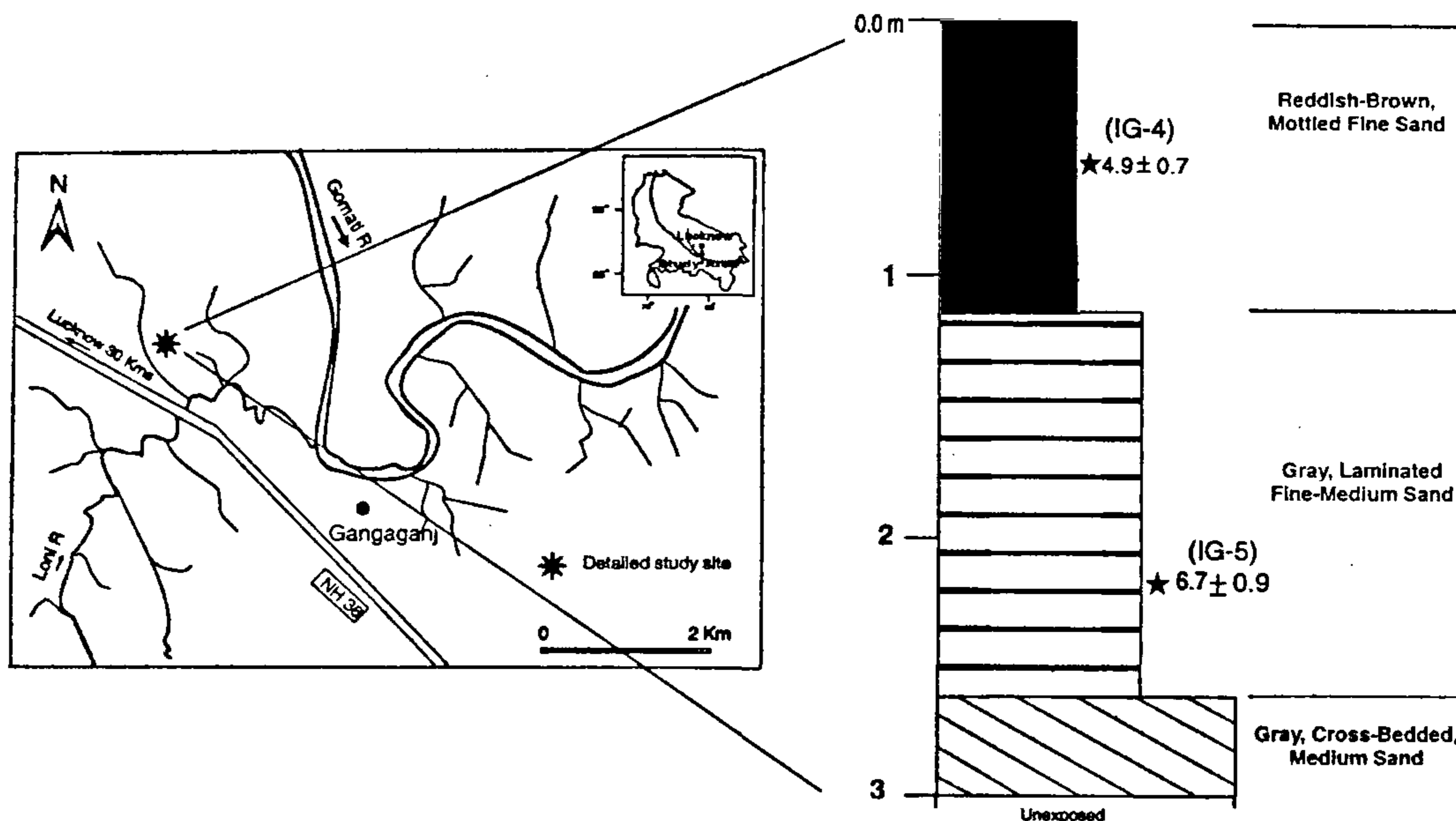


Figure 5. Location map, lithostratigraphy, and luminescence ages of Gangaganj ridge.

IRSL ages suggest that the channel was abandoned sometime between 7.2 and 4.9 ka.

In the case of the Gangaganj ridge, IG-5 has been dated to 6.4 ± 0.1 ka and IG-4 yielded an age of 5.0 ± 0.7 ka. This means that abandonment of the channel occurred between 7.4 and 4.3 ka (taking maximum age spans). Evidence of neotectonic activity has been cited as one of the causative factors for channel abandonment<sup>9</sup>. The similarity of ages from the Gahira bypass implies an age bracket of 7.4 and 4.3 ka for this activity and suggests that a decrease in rainfall may have contributed significantly to the decline of fluvial regime. Summarizing the chronology of Bhur sand deposits both at the Gahira bypass and the Gangaganj indicates a channel activity until 8–7 ka. This fluvial activity ceased sometime between 7 and 5 ka, and a phase of aeolian accretion occurred around 5–4 ka.

The upland interfluvial surfaces of the Ganga Plain witnessed several climatic changes<sup>3–5,17</sup> and neotectonic activities<sup>9,19–22</sup> during Late Pleistocene–Holocene. Singh<sup>5</sup> argued that many channels of the Ganga Plain are in different stages of decay due to decreased water budget in last few hundred to few thousand years. The present study places the onset of such a phase at ~ 5 ka. Studies from lake deposits of the Central Ganga Plain suggest decreased rainfall and increased aridity around 5–6 ka (refs 5, 11). Studies from the Arabian Sea<sup>23,24</sup> and SW Indian Ocean<sup>25</sup> demonstrated that the SW Indian monsoon was re-established during 14–11 ka and peaked at around 9 ka and subsequently a decline occurred around 5–4 ka. Studies from lakes in the Thar desert also show that most of the lakes in the area suffered desiccation around 5–4 ka due to weakening of the SW monsoon<sup>26</sup>. The overall similarity in record suggests

that the sedimentary record of the Gangetic Plain mimics the monsoon fluctuation, besides a tectonic component.

To conclude, the chronological and sedimentological data in the present study show that: (1) Fluvial activity in the interfluvial areas of the Central Ganga Plain existed during 8–7 ka which coincides largely with a phase of enhanced monsoonal precipitation. With this perspective it seems logical to suggest that initiation and/or reactivation of the fluvial channels on interfluvial areas should have occurred at around 13 ka, coinciding with the re-establishment of the SW monsoon activity at ~13 ka (ref. 24). (2) Abandonment of many of these channels took place during 7–5 ka, and aeolian activity at 5–4 ka resulted in ridge-like Bhur deposits. (3) A neotectonic activity was reported to be one of the causes for cessation of the channel process at Gangaganj<sup>9</sup>. This can be bracketed between 7 and 5 ka.

24. Sirocko, F., Sarinthein, M., Erlenkeusers, Lange, H., Arnold, M. and Duplessy, J. C., *Nature*, 1993, **364**, 322–324.
25. Elise Van Campo, *Quat. Res.*, 1996, **26**, 376–388.
26. Enzel, Y., Ely, L. L., Mishra, S., Ramesh, R., Amit, R., Lazar, B., Rajaguru, S. N., Baker, V. R. and Sandler, A., *Science*, 1999, **284**, 125–128.

ACKNOWLEDGEMENTS. UGC and CSIR, New Delhi are acknowledged for financial support to P.S., S.S. and M.S. The luminescence dating system was procured under a DST grant. U.K.S. thanks Head, Department of Geology, Kumaun University, Nainital for permission and support.

Received 14 September 1999; revised accepted 24 December 1999

1. Lyon-Caen, H. and Molnar, P., *Tectonics*, 1985, **4**, 513–538.
2. Parkash, B. and Kumar, S., in *Sedimentary Basins of India* (eds Tandon, S. K., Pant, C. C. and Casshyap, S. M.), Gyanodaya Prakashak, Nainital, 1991, pp. 147–170.
3. Singh, I. B., *Indian J. Earth Sci.*, 1987, **14**, 272–282.
4. Singh, I. B., in *Gangetic Plain: Terra Incognita* (ed. Singh, I. B.), Geology Department, Lucknow University, 1992, pp. 1–14.
5. Singh, I. B., *J. Palaeontol. Soc. India*, 1996, **41**, 99–137.
6. Singh, I. B., Srivastava, P., Shukla, U. K., Sharma, S., Sharma, M., Singh, D. S. and Rajagopalan, G., *Facies*, 1999, **40**, 197–210.
7. Khullar, V. K. and Gadhoke, S. K., *Rec. Geol. Surv. India*, 1992, **126**, 46–48.
8. Pandey, B. N., Bisaria, B. K. and Srivastava, A. B., *Rec. Geol. Surv. India*, 1992, **125**, 37–40.
9. Singh, I. B., Shukla, U. K. and Srivastava, P., *J. Geol. Soc. India*, 1998, **51**, 315–322.
10. Sinha, R., Friend, P. F. and Switsur, V. R., *Geol. Mag.*, 1996, **133**, 85–90.
11. Agarwal, A. K., Rizvi, M. H., Singh, I. B., Kumar, A. and Chandra, S., in *Gangetic Plain: Terra Incognita* (ed. Singh, I. B.), Geology Department, Lucknow University, 1992, pp. 35–43.
12. Aitken, M. J., *Thermoluminescence Dating*, Academic Press, London, 1985, p. 359.
13. Aitken, M. J., *An Introduction to Optical Dating*, Oxford Science Publications, New York, 1998, p. 267.
14. Gemmell, A. M. D., *Nucl. Tracks Radiat. Meas.*, 1985, **10**, 695–702.
15. Berger, G. W., *J. Geophys. Res.*, 1990, **95**, 12375–12397.
16. Rao, M. S., Bisaria, B. K. and Singhvi, A. K., *Curr. Sci.*, 1997, **72**, 663–669.
17. Botter-Jensen, L., Ditlefsen, C. and Mejdhal, V., *Nucl. Tracks Radiat. Meas.*, 1991, **18**, 257–263.
18. Prescott, J. R. and Hutton, J. T., *Radiat. Meas.*, 1994, **23**, 497–500.
19. Singh, I. B., Ansari, A. A., Chandel, R. S. and Misra, A., *J. Geol. Soc. India*, 1996, **47**, 599–609.
20. Singh, I. B., Rajagopalan, G., Agarwal, K. K., Srivastava, P., Sharma, M. and Sharma, S., *Curr. Sci.*, 1997, **74**, 1114–1117.
21. Singh, I. B. and Ghosh, D. K., in *India: Geomorphological Diversity* (eds Dikshit, K. R., Kale, V. S. and Kaul, M. N.), Rawat Publication, Jaipur, 1994, pp. 270–286.
22. Srivastava, P., Parkash, B., Sehgal, J. L. and Kumar, S., *Sediment. Geol.*, 1994, **94**, 129–151.
23. Overpeck, J., Anderson, D., Trumbore, S. and Prell, W., *Climate Dyn.*, 1996, **12**, 213–225.